NASA/TM–2020-5007323

Freestream Mach-Number and Temperature Measurement in NASA Langley's 20-Inch Supersonic Wind Tunnel Using Laser-Induced Thermal Acoustics

Gregory C. Herring, R. Jeffrey Balla, and George B. Beeler
Langley Research Center, Hampton, Virginia

September 2020

NASA STI Program . . . in Profile

Since its founding, NASA has been dedicated to the advancement of aeronautics and space science. The NASA scientific and technical information (STI) program plays a key part in helping NASA maintain this important role.

The NASA STI program operates under the auspices of the Agency Chief Information Officer. It collects, organizes, provides for archiving, and disseminates NASA's STI. The NASA STI program provides access to the NTRS Registered and its public interface, the NASA Technical Reports Server, thus providing one of the largest collections of aeronautical and space science STI in the world. Results are published in both non-NASA channels and by NASA in the NASA STI Report Series, which includes the following report types:

- TECHNICAL PUBLICATION. Reports of completed research or a major significant phase of research that present the results of NASA Programs and include extensive data or theoretical analysis. Includes compilations of significant scientific and technical data and information deemed to be of continuing reference value. NASA counter-part of peer-reviewed formal professional papers but has less stringent limitations on manuscript length and extent of graphic presentations.

- TECHNICAL MEMORANDUM. Scientific and technical findings that are preliminary or of specialized interest, e.g., quick release reports, working papers, and bibliographies that contain minimal annotation. Does not contain extensive analysis.

- CONTRACTOR REPORT. Scientific and technical findings by NASA-sponsored contractors and grantees.

- CONFERENCE PUBLICATION. Collected papers from scientific and technical conferences, symposia, seminars, or other meetings sponsored or co-sponsored by NASA.

- SPECIAL PUBLICATION. Scientific, technical, or historical information from NASA programs, projects, and missions, often concerned with subjects having substantial public interest.

- TECHNICAL TRANSLATION. English-language translations of foreign scientific and technical material pertinent to NASA's mission.

Specialized services also include organizing and publishing research results, distributing specialized research announcements and feeds, providing information desk and personal search support, and enabling data exchange services.

For more information about the NASA STI program, see the following:

- Access the NASA STI program home page at http://www.sti.nasa.gov

- E-mail your question to help@sti.nasa.gov

- Phone the NASA STI Information Desk at 757-864-9658

- Write to:
  NASA STI Information Desk
  Mail Stop 148
  NASA Langley Research Center
  Hampton, VA 23681-2199

NASA/TM–2020-5007323

Freestream Mach-Number and Temperature Measurement in NASA Langley's 20-Inch Supersonic Wind Tunnel Using Laser-Induced Thermal Acoustics

Gregory C. Herring, R. Jeffrey Balla, and George B. Beeler
Langley Research Center, Hampton, Virginia

National Aeronautics and
Space Administration

Langley Research Center
Hampton, Virginia 23681-2199

September 2020

Available from:

NASA STI Program / Mail Stop 148
NASA Langley Research Center
Hampton, VA 23681-2199
Fax: 757-864-6500

Freestream Mach-Number and Temperature Measurement in NASA Langley's 20-Inch Supersonic Wind Tunnel Using Laser-Induced Thermal Acoustics

G. C. Herring, R. J. Balla,

Advanced Measurement and Data Systems Branch

NASA Langley Research Center, Hampton, VA 23681

and G. B. Beeler

Flow Physics and Control Branch

NASA Langley Research Center, Hampton, VA 23681

Table of Contents

List of Figures

Abstract

We report single-laser-shot (≈ 0.3 μs) and time-averaged (500 laser shots at 30 Hz repetition rate) measurements of static temperature T and Mach number M in the freestream of NASA Langley's 20-inch Supersonic Wind Tunnel (SWT), using a nonintrusive optical technique: laser-induced thermal acoustics (LITA). Although the single-shot LITA T measurements show typical standard deviations (SD) of the sample of ± 4% (± 1-σ or 68% confidence for random errors), the 1-s averages show SDs of the mean ΔT = ± 0.5 K, or ± 0.3% for flow at T ≈ 160 K. The 17-s averages show ± 0.1% SDs of the mean. Both 1-s and 17-s averages agree to within about 1% of SWT's traditional probe measurements. Additionally, the single-shot LITA M measurements show typical shot-to-shot SDs of the sample of ± 5% (± 1-σ), but the 1-s averages indicate 1-σ SDs of the means ΔM = ± 0.02, or ± 1% for M = 2.0. Extending the time averages to 17 s, SDs of the mean are reduced to about ΔM = ± 0.007, or ± 0.4% (± 1-σ). The 1-s and 17-s time-averaged LITA-measured Mach numbers also agree with the SWT probe instrumentation to within 1%. Most of the shot-to-shot measurement noise probably arises from the LITA instrument itself (the fundamental limit of Fourier transforming a short-duration data series). Thus the 1-s averages only provide upper limits for the temporal stability of the freestream tunnel flow on 1-s time scales and complement previous work that characterized the SWT spatial uniformity of the flow. They also provide a first noninvasive comparison to the traditional calibrations with physical probes, for both the mean and fluctuating components of the freestream.

Nomenclature

E	Electric field strength
f_B	Main observed beat frequency = 2 $\Delta\omega$ in 3-beam LITA thermometry
f_1	First of two extra beat frequencies in 4-beam LITA velocimetry
f_2	Second of two extra beat frequencies in 4-beam LITA velocimetry
LITA	Laser Induced Thermal Acoustics
LO	Local oscillator laser beam for optical heterodyne detection
M	Flow Mach number = $(f_2 + f_1) / (f_2 - f_1)$ for supersonic flow, where $f_2 > f_1$
PMT	Photo-multiplier tube
P	Test-section freestream static pressure
P_t	Settling-chamber pressure = total pressure = stagnation pressure
SNR	Signal-to-noise ratio
SWT	NASA Langley's Supersonic Wind Tunnel
T	Test-section freestream static temperature
T_t	Settling-chamber pressure = total temperature = stagnation temperature
UPWT	NASA Langley's Unitary Plan Wind Tunnel
V_F	Flow speed
V_S	Speed of sound, where $V_s = (f_B / 2) \times \Lambda = \Delta\omega / \Delta k$
$\Delta\omega$	LITA soundwave frequency = frequency shift in Brillouin scattering
Δk	LITA inverse acoustic wavelength = $1 / \Lambda$
Θ	Full crossing angle of the two LITA pump laser beams
Λ	Wavelength of soundwave generated by the two crossed LITA pump beams
Ω_L	Optical frequency of the LITA probe laser ~ 10^{15} Hz
ρ	Flow static density
Φ	Full crossing angle between the transmitted probe laser beam and the Bragg reflected LITA signal beam ($\Phi / 2$ = crossing angle between LITA probe beam and the bisector of the two crossed pump beams)

I. Introduction

For good confidence in aeronautical ground testing, the flow conditions of the test facility should be well known. In this report, we present an update on the flow characterization of NASA Langley Research Center's (LaRC) 20-Inch Supersonic Wind Tunnel (SWT), a 2-dimensional (2-D), 20-inch-tall, variable-Mach-number supersonic tunnel, that was transferred to LaRC from Jet Propulsion Laboratory (JPL). After relocation from JPL to LaRC, SWT was rebuilt, modified, and recalibrated [1] circa 1986. Subsequently, some researchers have added to the original tunnel calibration [2], in the form of preliminary tasks, before proceeding on to their main research work of interest. For example, time-averaged freestream Mach number M was recently documented with a 1-D map using a Pitot probe [3], to characterize the spatial uniformity of the freestream, before undertaking the main task of studying boundary-layer transition on a swept wing.

One of SWT's long-term goals is a more extensive 3-D mapping of M over the test section, to add to the recent Pitot probe-based mapping. The SWT probe strut is restricted to a single line-of-sight in the test section, and so another method is necessary for 3-D mapping. Laser-induced thermal acoustics (LITA) is one method under consideration, and the work described in this report is a proof-of-concept of the use of LITA in SWT. Although not yet producing spatial maps during the short test window available, this preliminary work did result in data showing temporal fluctuations, complementing the previous characterizations of spatial nonuniformities. The data provide upper limits of Mach number and static temperature T fluctuations during a tunnel run, but only at a single freestream location.

LITA thermometry and velocimetry has been repeatedly demonstrated [4-21]. Despite its relatively lower signal, we chose a nonresonant version of LITA, because it does

not require seeding (i.e., a better quality of noninvasive measurement) and it has previously demonstrated the ability to measure subsonic [10] and supersonic [11-13] Mach number (w/o a calibration) with uncertainties (accuracy) of ≈ 1% or less. In SWT we anticipated better signal-to-noise ratios (SNR) due to the higher densities, compared to the earlier work [11-13] at NASA LaRC's Unitary Plan Wind Tunnel (UPWT). Compared to UPWT, a closed-circuit supersonic facility with compressors, we also anticipated smaller freestream flow fluctuations in the blow-down design at SWT, due to differences in the quiet-tunnel-inspired settling-chamber wall treatments.

With our previous relatively low-SNR LITA measurements at UPWT [11-13], only the low-noise 17-s averages were reported. Here, with greater SNR in SWT, we show 1-s average and single-shot results. Of the many versions of LITA velocimetry, we chose one [8, 20] that used a simpler version of optical heterodyning to accommodate the limited test window for this work. Note that we have demonstrated alternative and superior heterodyned-LITA versions for subsonic [10] and supersonic [11] flows that improve on the present results, but they are more labor-intensive and require more preparation and setup time.

II. The LITA Technique

Laser-induced grating techniques have been under development since the 1980's [14-18]. LITA methodologies can be divided into two general classes: those that generate traveling acoustic waves (acoustic gratings) from nonresonant electrostriction and those that generate predominately thermal gratings along with the acoustic gratings, from a resonant optical absorption in one of the sample's constituents. In this work, we use only the electrostriction approach to minimize the very small perturbation to the flow. There is no

direct optical absorption in the dry airflow (typically a dew point of -90 F) for our 1064-nm wavelength pump laser.

The LITA method of light scattering is schematically illustrated in Figs. 1a-1c. Two crossed beams at angle Θ, from a 10-ns pulsed pump laser, create a transient 10-ns optical interference pattern in the region of overlap (ellipsoid of ~ 0.5 mm by 1 cm). By electrostriction, this interference pattern instantaneously launches two, initially overlapped, counter-propagating acoustic plane wave packets, with wavelength Λ, into the gas medium (Fig. 1a, where the CW probe and LO beams are omitted for clarity of the pump process). The electrostriction force vector is proportional to ∇E. These wave packets travel perpendicular to the symmetry axis of the crossed beams. The lifetime of these transient wave packets is ~ 1 μs for the conditions at SWT, since they are absorbed by the gas and converted into heat. Illumination of the time-evolving density grating (from the two traveling wave packets) at angle Φ, with a second laser (the probe) at frequency Ω_L, temporarily scatters a small fraction (~ 10^{-6}) of the probe beam power for the lifetime of the gratings, where each wave packet scatters its own distinctive beam. This signal is in the form of a Bragg-reflected signal beam that consists of two overlapped and co-propagating components that are spectrally distinct (red and blue beams in Fig. 1b, where the the two pump beams are omitted for clarity of the interrogation process.). These two components are distinguished by different Doppler shifts $\pm \Delta\omega$ (i.e., the shift $\Delta\omega$ in spontaneous Brillouin scattering) determined by the counter-propagating geometry of the two wave packets. Electrostriction-based LITA is closely related to stimulated Brillouin scattering. In this case of simple optical heterodyning, the mixing of the two signals on the detector photocathode, at frequencies $\Omega_L \pm \Delta\omega$ (both at ~ 10^{15} Hz), produces a single modulation of this Bragg-

diffracted signal at beat frequency $\Delta\omega$. For our pump laser wavelength 1064 nm and crossing angle $\Theta \sim 1$ deg, $f_B = 2\,\Delta\omega \sim 20$ MHz and $\Lambda \sim 40$ μm. If the sound-wave reciprocal wavelength is Δk (i.e., wave vector difference of the two pump beams), the two Doppler shifts are $\Delta\omega = \Delta\mathbf{k} \bullet (\pm \mathbf{V}_S)$, where $\pm \mathbf{V}_S$ are the velocities of the two counter propagating wave packets and $|\pm \mathbf{V}_S|$ = the speed of sound (bold-faced quantities denote vectors).

Measurement of the beat frequency $2\,\Delta\omega$, with known grating wavelength $\Lambda = 1 / \Delta k$, yields the sound speed. If the mass composition of the fluid is known, translational static temperature T is then determined since $T \propto V_S^2$. An instrument calibration is required to find Λ (i. e., measuring the crossing angle Θ of the pump beams is the same as measuring the Λ of the acoustic wave packet) and is usually done with no flow when the temperature is confidently known. If the flow medium is in motion at velocity V_F (assumed to be parallel to Δk and V_S) and the temperature remains fixed, the frequencies of the signal beam are shifted to $\Omega_L + \Delta\mathbf{k} \bullet (\mathbf{V}_F \pm \mathbf{V}_S)$, but the beating at the difference frequency $2\,\Delta\omega$ is unchanged. Thus the beat frequency $2\,\Delta\omega$ changes only with temperature and not with velocity. So only temperature (not flow velocity) is detectable with this limited 3-input beam setup.

However, the bulk fluid motion at velocity V_F is readily obtained from a modification to the temperature-only version. With a classical (or traditional) heterodyne approach [8, 9, and 20], a fourth input beam (green beam in Fig. 1c, where the pump beams are omitted for clarity of the interrogation process), a local oscillator (LO) with no Doppler shift at the probe frequency Ω_L, with optimum intensity is introduced collinearly with the diffracted signal beams, and all three are incident on the detector. The local oscillator mixes nonlinearly with the two original signal beams on the detector. With this more-complicated optical heterodyning, the detected signal shows modulation at three frequencies (f_B, f_1, f_2): $f_B = 2\,\Delta\omega$

as before, and new signals $f_1 = |\Delta\omega| - (\Delta\mathbf{k} \bullet \mathbf{V}_F)$ and $f_2 = |\Delta\omega| + (\Delta\mathbf{k} \bullet \mathbf{V}_F)$. Here f_1 and f_2 are ≈ 10 and 30 MHz for Mach 2 flow parallel to the propagation axis of the sound wave packets. After the temporal waveform is digitized, and the three frequencies can be extracted by a variety of methods. The frequency $2\,\Delta\omega$ still gives V_S and T, again with a suitable calibration, while V_F is derived from the measured frequency difference, $2\,\Delta\omega'$, of the two new components, where $\Delta\omega' = \Delta\mathbf{k} \bullet \mathbf{V}_F$. Then $V_S = \Delta\omega / \Delta k$, $T \propto V_S^2$, and $V_F = V_S\,\Delta\omega' / \Delta\omega = \Delta\omega' / \Delta k$. Alternatively Mach number $M = V_F / V_S = \Delta\omega' / \Delta\omega = (f_2 + f_1) / (f_2 - f_1)$ for supersonic flow, where now a calibration of Δk is not required as it is for a temperature or absolute velocity measurements. The noise is reduced by the ratio computation of the sum and difference, reducing the overall measurement uncertainty. With this heterodyne approach, sound speed, temperature, and one component of Mach number (or fluid velocity) are determined simultaneously in a measurement time interval of ~ 1 μs following a single laser pulse. But the flow direction is not given with this approach.

A second method for deriving the parameters from the measured frequencies, one that does give flow direction, is to fit the data to a model of the LITA signal [e.g., 20 and 21] that generally requires assumptions. This requires having an accurate model and confidence in it, which is not always possible. To avoid potential problems with an uncertain model and the assumptions it uses, we choose to use straightforward discrete Fourier transforms to derive frequencies from the raw time-domain waveforms. If the time domain data is converted to frequency domain with a real Fourier transform (i.e. not a full complex transform with real and imaginary inputs), this approach works fine for most speeds. But for example, it has the disadvantage of trying to resolve two closely separated peaks f_1 and f_2 for slow subsonic flow or trying to resolve f_1 and f_2 from zero frequency and f_B, respectively, at Mach 1. In other

words, frequency peaks of interest for some flow conditions will sometimes lie on non-flat baselines arising from nearby interfering peaks, adding a potential systematic error to the analysis. This difficulty of non-flat baselines can be averted by using a third method: quadrature detection with two 90-deg-shifted raw data signals and a full complex Fourier transform [10]. This method also provides flow direction. But this quadrature option was not practically available due to lack of preparation time and special optics.

Furthermore, it is time consuming and difficult to maintain the delicate optical alignment with this classical version [20] of heterodyne detection. This type of classical heterodyne system includes an alignment of two collinear beams over long path lengths that is sensitive to vibrations in non-laboratory applications. Thus at LaRC, we previously developed a new common-path [10] heterodyne approach (the third method in the above paragraph) that has three advantages over the traditional collinear heterodyne method. The first is it greatly improves the robustness of classical heterodyned detection, valuable in challenging wind tunnel environments with moderate noise and vibration levels that more-readily misalign the beams. Even in benign laboratory environments, this advantage of the common-path design reduces the amount of repetitive alignment necessary with the classical heterodyne setup with an alignment that tends to drift out of optimum adjustment. Second, this method also provides directionality of the velocity measurement. In brief, this version works by imaging the moving gas density gratings onto a fixed Ronchi ruling, providing the same spectral information of the classical approach, plus flow direction. Third, as described and used in Ref. [10], this common-path design allows easy acquisition of two orthogonally shifted LITA signals to be used as input with a full complex Fourier transform. With this quadrature detection, the frequency peaks of the Fourier transforms lie on flat baselines and

give slightly more accurate frequencies. Again as in the traditional heterodyne approach described above, Mach number $M = (f_2 + f_1) / (f_2 – f_1)$ without a required calibration. It is expected that some fraction of the instrument system noise will be canceled by the ratio computation of sums and differences of the same frequencies, thereby improving the overall measurement uncertainty.

So the common-path approach to heterodyning has three advantages over the traditional collinear approach. Although the first advantage saves time and reduces workloads during the labor-intensive periods of the acquisition of significant amounts of data required during some wind tunnel applications, the initial setup of the common-path method requires more preparation time and special optics. These resources were not available for this first demonstration in SWT, and as mentioned above, we expected larger SNR for SWT compared to UPWT. Therefore we decided to forgo the quadrature-based common-path approach of [10 and 11], use the simple classical collinear approach of [8 and 20], analyze the raw waveform data with real Fourier transforms instead of full complex transforms, and determine frequencies from spectra with non-perfectly-flat baselines.

III. SWT Test Setup

SWT is a two-dimensional supersonic blowdown tunnel (typical run times of 300 s) with a rectangular-shaped test section (18 inches wide by 20 inches tall), that was configured for Mach-2 airflow in the present work. The flexible nozzle plates had not been adjusted since the work of Ref. [3], and so the present Mach-2 flow should be nearly identical to that described in Ref. [3], with M = 2.03. Additional details about this facility and the previous flow characterization can be found in Refs. [1-3], and citations therein.

A schematic of the LITA diagnostic is shown in Fig. 2, including the SWT wind-tunnel test section, the two lasers (pump and probe), and the fiber optic/photomultiplier tube (PMT) detection of the LITA signal. A magnified schematic of the details of the beam crossing region was previously shown in Fig. 1. The first laser is the LITA pump laser at 1064-nm, that is Q-switched with 10-ns pulses at a 30-Hz repetition rate. The beam is split into two LITA pump beams (25 mJ per pulse per beam), that are focused and crossed at a small angle (~ 1 deg) in the test section flow. The interference pattern in the ellipsoidal crossing region (≈ 0.5 cm along the beam-travel direction, by ≈ 0.5 mm transversely) and the short 10-ns pulse duration combine to, effectively instantaneously, launch two counter-propagating sound-wave pulses transverse to the beam directions. Initial sizes and pulse-widths of the sound-wave packets, before they have had a chance to propagate significantly, are determined by the focused pump-beam geometry.

Since a complete measurement can be made for every 1064-nm laser pulse (repetition rate 30 Hz), averaging multiple pulses gives time-averaged data of duration of the number of pulses times 0.033 s. Here both 1-s and 17-s averages (averaging 30 and 500 shots respectively) are presented. LITA data was acquired as ≈ 17-s long data-streams of 500 laser shots, where the analog LITA signal voltage was digitized 2000 times at 1-ns intervals for each laser shot. Each set of 2000 samples is approximately centered on the 10-ns pump laser pulse by a pump-laser trigger pulse and pulse delay generator. Each 17-s, 500-laser-shot LITA data-stream is labeled as a single LITA point and numbered. The LITA system put together for this demonstration could acquire only two separate 500-shot data-streams during a 60-s SWT run. Often throughout this document, the terminology LITA Point # to refer a

single LITA data-stream of 500 laser shots (17 s long), whether 500 single shots, seventeen 1-s averages or a single 17-s average is displayed.

The narrow-band continuous wave (CW) seeder laser, that narrows the linewidth of the LITA pulsed pump laser at wavelength 1064 nm, was not used for this experiment. The climate control system was partially broken for the time window of the present test and the temperature and humidity of the facility room were not as well controlled as usual. The resulting variations of climate in the SWT facility room seemed to affect the quality of the seeding, and, to a lesser degree, tunnel vibrations from wind-on intervals also seemed to influence the seeding quality. Part of the cause of the unreliability of the seeder laser may have been due to the advanced age of this seeder. To reduce the possibility of seeder-based pump laser variations (i.e. additional instrument noise) in the middle of LITA data-stream acquisitions, we did not use the seeder in the current work; all results presented in this report are for the unseeded 1064-nm YAG output with a broadband averaged linewidth of about 1 cm^{-1}. Although the LITA instrument worked fine without the seeder, it is probable that use of the seeder would have improved the present LITA results by a small degree.

The second laser is the LITA probe laser at 532-nm, with CW emission that is also split into two beams, the upper probe-laser beam shown in Fig. 2 is called the probe and transits the crossing region at the Bragg angle for constructive reflectivity. A small fraction ($\sim 10^{-6}$) of this probe beam is Bragg-reflected off each of the two sound waves as an optical signal into the detection fiber optic. The acoustic wave packet lifetimes are limited to ~ 1 μs by pressure-dependent non-resonant acoustic absorption of the gas for no-flow and slow subsonic speeds. Displacement of the sound packets from the probe beam by the mean flow starts to limit the signal lifetime for supersonic speeds. These two effects combine to give

typical single-shot LITA signal durations that are ≈ 1 μs for 1-atm room conditions with no flow and ≈ 0.3 μs for Mach 2 at SWT (~ 0.2 atm static pressure P). Since the two sound waves travel in opposite directions, the Doppler shifts of the two reflected signals beams are different, and thus the square-law detector sees a beat frequency of the difference of the Doppler shifts. This beat frequency of ~ 20 MHz directly gives the sound speed. Since the gas composition is known, the gas temperature then depends on the square of the sound speed (or beat frequency) and an instrument calibration in a no-flow condition.

To measure temperature, only three input beams are needed: the two pumps at 1064 nm and the probe (upper 532-nm beam in Fig. 2). To measure Mach number, a fourth input beam (the lower 532-nm LO beam in Fig. 2) is introduced to propagate exactly down the path of the expected Bragg-reflected LITA signal from the probe beam. This fourth beam acts as a LO, representing a no-flow no-Doppler-shift reference. The three beat frequencies that now appear in the signal give again temperature and one component of flow velocity, that require a no-flow calibration, and now Mach number without a required calibration. In both cases (with or without the presence of the LO), the Bragg-scattered LITA signal is generated in the crossing region and travels down the path of the LO to the fiber optic input. If the LO is present, then the LITA signal beam is perfectly collinear with the LO beam.

LITA analog signal voltages and other relevant data were digitized and stored on a digital-storage oscilloscope (500-MHz analog bandwidth) before downloading to a computer. No explicit high-pass filter was used at the input to the oscilloscope for anti-aliasing purposes, thus the ~ 300-MHz roll-off of the PMT (50-ohm load) acted as a limiting high-pass filter. The high voltage between the PMT cathode and the first dynode was gated at 100 μs per pump laser pulse to minimize the possibility of saturation and stress on the PMT. All

analysis was done during post processing, using zero padding. Frequency spectra were calculated with the fast Fourier transforms (FFT) routine in LabVIEW, where no windowing was used, i.e., the same as using a rectangular (also called flat-top) window.

IV. LITA Results at SWT and Discussion

Temperature

LITA temperature results from SWT are shown in Figs. 3-7. Fig. 3 shows a typical single-laser-shot LITA waveform that lasts about 0.3 μs, for SWT Mach 2 flow. The static pressure and temperature (P and T) of the flow are 0.22 atm (3.2 psi) and 162 K (292 °R) respectively, while the tunnel stagnation conditions are labeled with a subscript "t" in the figure. This data is an example for a measurement of temperature only. It did not include the fourth input beam, the LO, and thus only one beat frequency at $f_B \approx 20$ MHz is apparent. For a no-flow 1-atm calibration point, at room temperature, the frequency will increase to ≈ 25 MHz, and the waveform will have a better SNR than that shown in Fig. 3. Temperature is determined from this measured frequency as described in Section II. Due to the variety of units used in this document, Table 1 summarizes the run conditions, in different units, for the data of Figs. 3-6 and 9. The first column contains conditions for two different LITA points, while each of the last four columns contains only one LITA point. The SWT flow conditions were originally recorded in psi for pressures and °F for temperatures.

Table 1: Run Conditions for Data of Figs. 3-6 and 9

Figure #	**3, 4, 5**	**6a**	**6b**	**6c**	**9**
Flow	Mach 2	Mach 2	No Flow	No Flow	Mach 2
SWT Run #	8	5	n/a	n/a	13
LITA Point #	20, 21	12	17	11	40
P_t (MPa)	0.18, 0.17	0.072	n/a	n/a	0.17
P_t (atm)	1.73, 1.65	0.71	n/a	n/a	1.66
P_t (psi)	25.5, 24.2	10.5	n/a	n/a	24.4
T_t (K)	291, 296	307	n/a	n/a	311
T_t (°R)	525, 534	552	n/a	n/a	561
T_t (°F)	64, 74	92.3	n/a	n/a	101
P (MPa)	0.022, 0.021	0.0092	0.027	0.101	0.021
P (atm)	0.22, 0.21	0.091	0.27	1	0.21
P (psi)	3.26, 3.09	1.34	4	14.7	3.12
T (K)	161, 164	170	295	298	173
T (°R)	291, 296	307	531	537	312
T (°F)	-169, -164	-153	71.2	77	-148

(note: 1 atm = 14.70 psi = 0.1013 MPa = 1.013 x 10^5 N/m^2)

A Mach-number measurement, that would include the addition of the fourth input laser beam, would look much the same as the trace of Fig. 3, but would exhibit a small-amplitude "modulation" of the main 20-MHz frequency, at $f_1 \approx 10$ MHz and a higher-frequency component at $f_2 \approx 30$ MHz. At SWT, the Mach-number data exhibited less SNR than shown in Fig. 3. Although not easily visible by eye in the temporal waveforms, because of the lower SNR, the 10 and 30-MHz components are better seen in the Fourier transforms

of the raw waveforms. Temperature and Mach number are then determined from these three measured frequencies as described in Section II.

The fast-exponential decay of the sinusoidal oscillation shown in Fig. 3 is the combination of acoustic absorption (amplitude $\propto$ frequency^2 $(T)^{1/2}$ / P) [22], the focused beam size and crossing angle, and the mean flow sweeping the acoustic wave packets out of the probe beam before the absorption has fully attenuated the wave packet. Temperature is determined from a Fourier transform of the temporal waveform and a pre-flow calibration that consist of taking a LITA dataset with no-flow and a well-known temperature. This calibration effectively measures the crossing angle of the two LITA pump beams, that is then used for subsequent measurements (e.g., data of Fig. 3) with unknown temperatures. This calibration must be repeated anytime the LITA pump beam crossing angle changes.

To illustrate the temporal behavior of the airflow for a typical SWT run, Fig. 4 shows several SWT-facility data-streams from Run 08 of Test T2020. In the upper graph, the relative values of four recorded facility parameters are plotted on the same arbitrary scale, that shows air flow for about 200 s, of which the 100-s interval from time = 580 to 680 s labeled on the abscissa is the usable test flow. The first 100 s, from time = 480 to 580 s, is required to bring the air flow on point to the requested test condition. The yellow curve shows total pressure P_t, while the red and blue curves show the two total temperatures T_t from two different thermocouples (TC), all measured in the stagnation (settling) chamber. The gray curve shows the Mach number, that is measured with the traditional approach of comparing simultaneous measurements of freestream pitot pressure and stagnation-chamber pitot pressure measurements, and an assumed adiabatic expansion. In this upper graph, the

two red, doubled headed arrows show the locations of the two 17-s LITA data-streams (labeled LITA Points 20 and 21) that were acquired during the run.

The two lower graphs of Fig. 4 each shows all 500 measured frequencies of LITA Points 20 and 21, where each plotted symbol (gold open circles) consists of a single-laser-shot result. In these two graphs, Fourier transforms have already been performed on the raw LITA temporal waveforms of each shot, so that the resulting observed peak beat frequency can be plotted on the ordinate axis. The standard deviation (SD) of the 500-shot samples is about ± 2% (± 1-σ or 68% confidence for random errors). These fractional precision estimates will double when the frequencies are converted to temperature, since flow static temperature is proportional for LITA frequency squared. The blue triangles show a running 30-laser-shot smooth to illustrate what 1-s data averages would look like. These frequencies will be converted to temperature in Fig. 5. Three reasonable speculations as to the cause of this shot-to-shot noise is, in order of speculated importance, are (1) the fundamental Fourier limit of transforming short-duration waveforms like that shown in Fig. 3, (2) changes in the beam-crossing angles from wind tunnel vibrations, and (3) changes in the beam-crossing angles due to the beam-pointing variations, that occur in both of the LITA lasers.

Fig. 5 shows the same LITA data as shown in Fig. 4, except for two changes. First the frequencies of ≈ 19 MHz have been converted to temperature using a no-flow LITA calibration measurement made on the same day, after the pump beam crossing angle was no longer being adjusted. Second both LITA Points 20 and 21 have the 500 frequency measurements reduced to 17 measurements by averaging over sequential 30-shot segments. The precision of each plotted point is estimated as the SDs of the mean = ± 0.5 K (± 1-σ), or ± 0.3% for the flow at ≈ 160 K. Each plotted LITA symbol (filled blue and green circles) in

Fig. 5 is a 1-s average (like the running 1-s smooth shown in Fig. 4) and shows how the LITA temperature result varies over a 17-s data-stream on a 1-s time scale. The LITA data from Point 21 starts acquisition about 20 s after completing the acquisition of the data for Point 20, during a single 60-s SWT run. But the two points are plotted for convenient comparison on a common time frame on one graph, due to the fortuitous slight difference in absolute temperature at the two different time intervals of that particular run. For each of the two LITA data-streams, the SWT-facility-derived temperatures (crosses connected by a solid curve) from an average of the two TCs in the stagnation chamber and assuming cooling from a Mach-2 isentropic expansion are also plotted. One TC is located 1 ft from the bottom, and one is located 1 ft from the top of the ≈ 8-ft diameter stagnation chamber. These TCs are positioned downstream of the anti-turbulence screens, by more than 100 times the screen-wire opening. The SWT facility temperatures are also sampled at 1-s intervals. LITA stream 20 shows excellent average agreement with the facility-derived temperature, while the ≈ 1.5-K (3 °R) difference between LITA and SWT temperatures of Point 21 was typically the largest deviation that were observed when the LITA instrument was optimally calibrated (i.e., data for Day 1 only). These differences are equivalent to ± 1% for the freestream static temperatures or ± 0.5% of the stagnation temperatures. Whether or not the true flow temperature time histories look more like the LITA profiles or the SWT-stagnation-chamber-derived profiles will require further work with multiple in-situ diagnostic techniques, with 1-s or less time resolution.

One question that arises when looking at the LITA measurement results of Figs. 4 and 5 is, “How much of the observed noise in the LITA data is from the LITA instrument as opposed to being real flow fluctuations of the freestream flow?” This question is answered

by looking at the three data sets in Fig. 6. Figure 6 shows three different LITA data points for three different gas conditions. The flow conditions of the data of Fig. 6a (LITA Point 12) are similar to those of Figs. 4 and 5. Each of the three LITA points shows a 17-s history of 500 laser shots, where a Fourier transform is performed on each individual laser shot to determine frequency. These data are used to help evaluate the relative contributions of true flow fluctuations and the LITA-instrument noise to the observed total LITA noise, as decribed in Section IV.

Note the absolute values of the uncertainty levels of the three data sets, accounting for the differences in all the ordinate scales for Figs. 4, 5, and the three parts of Fig. 6. One direct observation of Fig. 6 is that the absolute noise levels are the same for the Mach-2 flow at ≈ static pressure 0.091 atm in part (a) and the no-flow at a pressure 0.27 atm in part (b). Because the flow is expanded and cooled to reach Mach 2, the gas conditions of Fig. 6a are three times less pressure and two times less temperature than for Fig. 6b. Since the LITA signal level roughly scales as P^2 / T^3 [23], these two data sets are expected to have roughly the same size signal: net change in signal level for the flow data relative to the no-flow is ~ $(P_1 / P_2)^2 / (T_1 / T_2)^3 \sim (1 / 9) / (1 / 8) = 8 / 9 \approx$ unity. The noise of Fig. 6b has only no-flow fluctuations and hence is all LITA instrument noise. Since the noise level of Fig. 6a (with flow) is the same as that in Fig. 6b (no-flow), the flow noise is mostly or all LITA-instrument noise. This is the first and main argument that suggests that the noise on the runs with flow is dominated by the LITA instrument noise.

A second way to look at the noise comparison of Figs. 6a and 6b is to note that the signal decay times and hence the frequency uncertainties are about the same, since both signals occur at relatively low pressure. And since we expect similar signal levels as noted

just above, the SNR levels should also be similar (which is roughly what is observed in Fig. 6) if the noise level is dominated by the instrument. Two other weaker arguments can be made by comparing Figs. 6a and 6c, and comparing 6b and 6c, but we omit the details since the first argument above is all that is necessary to form a reasonable conclusion.

Thus we argue that the residual noise on the single-shot LITA data does not illustrate the true flow fluctuations; the observed noise is essentially all LITA-instrument noise. Then we cannot assign a finite number to the temperature fluctuations of the SWT Mach-2 flow on time scales of ~ 1 μs. What about the 1-s averages? For the 1-s averaged data, we do not have enough data to make the same rough arguments as above. To be conservative, here we simply state that the 1-s averaged LITA results of Fig. 5 can be taken as upper limits for the freestream flow fluctuations (≈ 0.7%) of temperature in SWT on time scales of 1 s. On the other hand, the true flow fluctuations are probably not as small (~ 0.1 °R / 300 °R = 0.03%) as the extremely smooth SWT TC data of Fig. 5, due to the utilized TC time constants that approach ~ 1 s. Additional work is necessary to confidently assign a finite number (with uncertainties) to the fluctuations of static temperature in the SWT freestream flow. At longer time scales of 15-30 s, as the tunnel flow slightly heats or cools (as seen in Fig. 4), there is excellent agreement between the LITA and SWT data, for the relative temperature changes of ~ 2 °R.

A summary of all temperature measurements made in a single day (Day 1) with four SWT runs and eight LITA points (two 17-s LITA points or data-streams per SWT run) is shown in Fig. 7a. The absolute LITA temperature values are determined by a single no-flow data-stream (with 4 psi pressure in the test section) acquired typically early in the day (before running), using a single TC-measured room-air temperature located just outside (external) of

the test section. If the beam alignment changes and requires realignment, a new calibration for future data is necessary. Thus the LITA absolute temperatures with the present procedure are ultimately based on a TC calibration. Although the LITA SDs (precisions) of 500-shot means are ± 0.1%, we see anywhere from "perfect" agreement (i.e., difference less than the LITA precision) to small differences of ≈ 1% when the LITA temperatures are compared with the SWT facility temperatures derived from the stagnation chamber TCs and assuming Mach-2 isentropic cooling. Even if the calibration TC is located outside of the test section (as was the case for Day 1), excellent results can be obtained if the test section gas, physical structure of the test section, and the room air are all in good thermal equilibrium. With the small differences of 1% or less, again, additional work is necessary to decide whether it is the LITA or SWT probe values (or neither) that are truly correct.

Data from two more days are shown in Fig. 7b, along with the data of Fig. 7a for comparison; note the change in the vertical temperature scale in Figs. 7a and 7b. The three days of data in Fig. 7b show all the temperature data from the entire test, in the form of 17-s averages (each plotted symbol is a 500-laser-shot average). The calibration for Day 1 was taken with the test section at 4 psi, approximately the static pressure of the test section when the tunnel is running at Mach 2 and Pt = 15 or 25 psi, whereas the calibration for Day 3 was taken with the test section at 14.7 psi (1 atm) pressure.

To improve the quality of the LITA calibration, on Day 2, a different thermocouple was used to calibrate the LITA data, one that was located inside the test section and mounted on the SWT probe strut, much closer to the LITA sample volume. However, the next day, it was discovered that the probe-strut TC was partially malfunctioning and not reliable. This is the reason for the ≈ 10% discrepancies of the Day-2 LITA data with the facility data. On a

third day, Day 3, we switched back to using a TC external to the test section, for the calibration. In addition, on Day 3 we were forced to unexpectedly quit working without a low-pressure calibration (i.e., test section at ≈ 4 psi); however we did have a calibration at room pressure of 14.7 psi. Taking the calibration with a reduced pressure (~ flow static pressure) inside the test section is important, since the pressure difference on the large tunnel doors can minutely flex the doors, move the door-mounted windows that allow the laser beam ingress and egress to the test section, and potentially change the crossed-beam alignments. We speculate this 1-atm calibration is responsible for the ≈ 2% discrepancies between the LITA-derived and the facility probe-derived temperatures on Day 3.

To be clear the data on Day 2 is outright wrong (because of the calibration TC failure) and are not usually included in formal reports. We do not consider the data from Day-2 or Day-3 to be high-quality data that would be included in final research-related conclusions. We show this subpar data in this developmental effort, in the spirit of showing all the data and for another reason. These calibration problems on Day-2 and Day-3 illustrate how important the TC calibration is for LITA thermometry. We have previously demonstrated an alternative and superior method [20] for deriving absolute temperatures from LITA, using a simultaneous dual-LITA setup that reduces the sensitivity to the calibration. It utilized two independent LITA systems running simultaneously, one with a temperature-stabilized reference cell that is used as the very-well-known-temperature calibration for use with the unknown-temperature LITA signal from the test sample. This alternative also reduces the statistical noise due to the approximately random beam-crossing fluctuations. Thus this dual-LITA system improves the data in two ways, one related to the precision and one related to the accuracy. But this dual-LITA system is more complicated, requires more equipment and

time-intensive care taking; hence it is also costlier. The dual LITA methodology is the preferred strategy if the resources are available but was not pursued here due to the limited resources and time.

Mach Number

Only temperature results have been discussed above, but Mach-number mapping is a more important goal for the SWT facility characterization. In this section, we discuss a preliminary demonstration of Mach-number measurements in SWT with LITA, illustrating the quality of the data possible with the particular setup used here. The SWT facility Mach number was calibrated before the time frame for the present LITA measurements, but the flexible-wall settings were not adjusted between the previous calibration and the present LITA measurements. The expected [3] tunnel condition was Mach 2.03 ± 0.003 (the mean was measured, and the uncertainties were estimated for the probe determinations of Mach number in Ref. [3]). This facility Mach number was measured from the ratio of Pitot probe total pressure measurements from the test section and simultaneous pitot pressure measurements in the stagnation chamber. The pitot probe is mounted on a translatable strut, and multiple spatial locations along a line can be observed. The Pitot probe measurements from Ref. [3] were typically made ~ 5 cm above the LITA sample region and were averaged for 1 s. Fig. 8 of Ref. [3] shows a sample of the expected small ($\Delta M = \pm 0.02$) spatial variation of time-averaged Mach number over the spatial region accessible by the probe strut. The present LITA measurements are confined to a single centerline location.

As background, the temperature measurements above come from the measured beat frequency from optical heterodyning of the two signal beams (red and blue in Fig. 1b)

reflected from the two acoustic wave packets. As described in Section II, a fourth input laser beam (labeled LO in Fig. 2) needs to be added to the sample region to make a LITA Mach-number measurement, by measuring three beat frequencies from optical heterodyne detection of these two signals and a LO (green beam in Fig. 1c). Vibration of laser beams is a typical problem to overcome for many laser experiments, especially for heterodyne methods that essentially make use of an optical interferometer. Section II also notes why we did not use a common-path method that is effective against environmental vibrations. Here we tried a simpler vibration-reduction technique, one that could be implemented in a short time frame.

Fig 8 schematically illustrates three strategies for implementing heterodyne detection. The first, option (1), the traditional or classical one, has long been used in the literature and recently for LITA by others [8 and 9] and us [20]. We have previously demonstrated a second strategy, option (2), a superior common-path approach [10] that reduces vibration effects, but it was decided to not use it here to speed up the laboratory preparation time and the setup time in the wind tunnel. Thus for this initial SWT work, we decided to try a third strategy, option (3), because somewhat by chance, we already possessed the necessary special optic. This effort incurred only a small time-penalty to minimize the detrimental effect of tunnel vibrations on the beam crossing alignment, that reduces the LITA SNR.

This third strategy is also a classical heterodyne approach, but with a minor change to the beam splitting. The idea is to use a single thick optic to split off the LO beam from the probe beam as in option (3) of Fig. 8, instead of using a traditional beam splitter composed of two independent optics as shown in option (1). The small residual disadvantage of option (3) is that there is only one practical useable thickness of the single-splitter optic. One cannot use just any thickness optic. However, with the proper thickness and the setup of option (3),

the motion of the LO beam relative to the probe beam should be reduced compared to the setup of (1); hence phase variations between the signal and the local oscillator should be reduced and less noise observed on the signal. Extending this idea to split the pump laser beam into two LITA pump beams should also result in less relative pump beam movement due to vibrations, but this was not pursued in the present work because the exact specific optic was not readily available.

As an aside, an improved LITA instrument of the future might consist of two single-optic beam splitters - one to generate the two pump beams from a single pump laser, and one to generate the probe and LO beams from a second single probe laser. However, here due to availability of optics, we used this single-optic beam splitting method only for the probe and LO splitting as shown in option (3) of Fig. 8. We used a traditional two-optic splitter to split the pump into two pump beams, as shown in option (1) of Fig. 8.

Returning to the discussion of the present data, Fig. 9 shows a single 17-s segment of LITA-measured Mach number, after modifying the LITA apparatus used to acquire the temperature data from Figs. 3-5, by adding the fourth input laser beam to the setup. The data of Fig. 9 is from a different day than the days of Figs. 3-5. Each displayed symbol is a 1-s average (30 laser shots or somewhat less). As also noted in Fig. 9, The 30-laser-shot 1-s averages typically contain only about 20 measurements, since about 10 shots per 1-s period were not analyzable because the SNR was lower than for the above temperature measurements and thus the FFT results were ambiguous. Possibly these ≈ 10 bad shots can be salvaged for use with additional programming, rather than simply calling a commercially-available FFT routine as we did here. Here we simply throw away those ≈ 10 poor shots, but

the other ≈ 20 shots give a generally good 1-s average (although now these 1-s intervals are not perfectly uniformly sampled every 0.033 s).

One reason for the poorer quality SNR for the Mach-number measurements is that for the day of the data in Fig. 9, we did not get an opportunity to set the probe beam slightly (~ 1 beam diameter or less) downstream of the pump beams, as should be done for optimal signal generation (e.g., see Ref. [11]). All data presented here are without the probe beam translated downstream. Thus one unanticipated demonstration of the present work is that decent (~ 1% uncertainty) Mach-number measurements can be made in supersonic flow without translating the probe beam downstream of the pump beam crossing region, as was done in Ref. 11. This beam translation makes the alignment more difficult.

Black symbols in the left-hand panel show single-shot results, uniformly scattered (≈ ± 5% for 1-σ or 68% confidence limits) around the nominal expected value Mach 2. The blue diamonds in the right-hand panel show the 1-s average results. The 1-σ uncertainties for the 1-s averages are plotted as blue squares, near zero, in the right-hand graph and are about 1% of the mean Mach number of 2. As indicated by a red triangle and noted in red, the 17-s average gives a Mach number of 1.992 ± 0.006, where this uncertainty is ± 1-σ confidence for the mean. A second 17-s average measurement made about 20 s after the first 17-s set illustrated in the figure, during the same run, gave 1.997 ± 0.007, as annotated in green on the figure. This is to be compared to an apparently oscillating local mean Mach number that varies spatially from 2.01 to 2.05, derived from probes [3]. Our purely statistical uncertainties of ± 0.006 are twice the estimated uncertainty of [3], while our mean is about 1.5% lower. However the location of the two measurements differed by several centimeters or more, and this difference is similar to the oscillating spatial variation reported in [3].

V. Summary

We present single-laser-shot (0.3 μs) and time-averaged (30 shots at 30 Hz repetition rate) measurements of static temperature and Mach number in the freestream of NASA Langley's 20-inch Supersonic Wind Tunnel (SWT), using a nonintrusive optical technique: laser-induced thermal acoustics (LITA). The 1-s temperature averages show 1-σ (± 68%) standard deviations (SD) of the mean of ± 0.5 K for flow at ≈ 160 K. The 1-s Mach averages indicate 1-σ SD of the means of ± 0.02 for nominal Mach number 2, while the 17-s average reduce the 1-σ uncertainties to about ± 0.007. Both 1-s and 17-s averages generally agree to within ≈ 1% with SWT's traditional facility calibrations, for both temperature and Mach number.

For 160-K supersonic flow, LITA temperature measurements show ± 4% variations (1-σ) for single-laser-shot measurements (essentially all instrument noise due to the limit of the Fourier transform of short-duration signals), ± 0.3% precision (1-σ) for means of 1-s averages (30 laser shots), and ± 0.1% precision (1-σ) for the means of 17-s (500 shots) averages. For both 1-s and 17-s LITA averages, comparing to the TC-measured stagnation conditions, and assuming isentropic cooling due to Mach 2 expansion, we observe agreement to within ≈ 1% for the two absolute temperature determinations. These 1% differences can be taken as a first estimate of the LITA accuracies, if the SWT probe-based calibrations are taken to be correct. The total uncertainty for the 1-s measurements is a quadrature addition of the precision and accuracy ≈ $\sqrt{[(1)^2 + (0.3)^2]} \approx 1\%$.

There are very few in-situ measurements (including probes or non-invasive optical techniques) of the freestream static temperature for SWT. The typical way to measure freestream temperatures is by assuming adiabatic expansion of the settling-chamber

measurements using the measured Mach number. As discussed in Section IV, taking the settling-chamber-based values to be correct is just a simple and conservative method for a first assessment of the LITA accuracies. More realistically, additional work is needed to decide which measurement is more accurate for the small differences of ~ 1%.

For nominal Mach-2 flow, LITA Mach-number data have typical variations of ± 5% for single-laser-shots, ± 1% for 1-s averages (30 shots), and ± 0.4% for 17-s (≈ 300 shots). All these Mach-number LITA uncertainties are 1-σ precision values for the means. The nonintrusive LITA Mach-number measurements agree with the nominal SWT facility Mach number to within ± 1% for 1-s averages and to within ± 0.4% for 17-s averages. Again taking the SWT probes to be correct, these differences can be used as an estimate of the LITA accuracies, and the total uncertainty for the 1-s measurements is ≈ 1.4%, after adding the two errors in quadrature as $\approx \sqrt{[(1)^2 + (1)^2]} \approx 1.4\%$. The nominal SWT Mach numbers are derived from Pitot probe stagnation pressure measurements in the test-section and simultaneous static-pressure measurements in the stagnation-chamber. These LITA measurements are the first spatially-resolved, nonintrusive determinations of Mach number for the SWT facility.

Since most of the optical measurement noise probably arises from the LITA instrument itself (i.e., single-shot measurements that require Fourier transforming a short temporal waveform of ~ 1 μs), the shot-to-shot LITA noise is not yet relevant from a facility point-of-view. However, the averages provide reasonable upper limits for the stability of the freestream tunnel flow on their respective time scales. The present LITA results show that SWT flow has temporal fractional fluctuations of ≈ 1% (or less) on a 1-s time scale. These

results complement previous work [3] that has characterized the spatial uniformity for Mach number (also about 1%).

The present LITA results demonstrate near 1% uncertainties for both accuracy and precision, for both temperature and Mach number, for averaging times of 1 s. To make this claim for accuracy, we are taking the SWT probe calibrations to be the true values, although the probes are intrusive. This LITA-based work provides a first noninvasive measurement for comparison to the physical-probe calibrations and illustrates remarkable agreement for the mean component of the freestream flow at SWT.

Finally as summarized in the last sentence of Section II, the particular version of LITA that was employed here [20], due to time constraints, is a non-optimum classical heterodyne approach; use of the common-path heterodyne approach of Ref. [11] should improve on the present results. In addition, the pump laser was a multi-mode broadband output; use of a seeded, narrow-band version should also improve the present results. Third we did not use a dual-LITA setup for best quality calibration data; use of a dual-LITA calibration should also improve upon the present results. So one might speculate that any future LITA work at SWT could obtain better quality results than those presented here, if any of these three improved strategies were used. However facility vibrations should also be considered. Although in this work at SWT, vibrations were not generally a factor, an important exception was when the settling-chamber pressure remained at P_t = 20 psi for too long (> ~ 5 s), where the SWT structure apparently has a strong vibrational resonance at this pressure. For this situation, the resulting resonant vibration completely misaligned the LITA system to the point of eliminating the entire signal.

VI. Acknowledgements

Many thanks are extended to W. G. Culliton, M. T. Fletcher, M. A. Kulick, and J. W. Werner for help with different aspects of this work.

VII. References

1 J. L. Dillon, R. L. Trimpi, and A.E. Schultz," The NASA-Langley 20-Inch Supersonic Wind Tunnel," AIAA Paper 86-0765 (1986).

2 J. L. Dillon, R. L. Trimpi, and F. J. Wilcox, "Unexpected Results from the Langley 20-Inch Supersonic Wind Tunnel During Initial Checkout," AIAA Paper 88-1999-CP (1988).

3 L. R. Owens, G. B. Beeler, and P. Balakumar, "Flow Disturbance and Surface Roughness Effects on Cross-Flow Boundary-Layer Transition in Supersonic Flows," AIAA Paper 2014-2638 (2014).

4 R. B. Williams, P Ewart, and A. Dreizler, "Velocimetry of Gas Flows Using Degenerate Four-Wave Mixing," Opt. Lett. **19**, 1486-1488 (1994).

5 E. B. Cummings, H. G. Hornung, M. S. Brown, and P. A. Debarber, "Measurement of Gas-Phase Sound Speed and Thermal Diffusivity Over a Broad Pressure Range Using Laser-Induced Thermal Acoustics," Opt. Lett. **20**, 1577-159 (1995).

6 P. Barker, J. H. Grinstead, and R. B. Miles, "Single-Pulse Temperature Measurement in Supersonic Air Flow with Predissociated Laser-Induced Thermal Gratings," Opt. Comm. **168**, 177-182 (1999).

7 M. S. Brown and W. L. Roberts, "Single-Point Thermometry in High-Pressure Sooting, Premixed Combustion Environment," Journal of Propulsion and Power **15**, 119-127 (1999).

8 S. Schlamp, E. B. Cummings, and T. H. Sobota, “Laser-Induced Thermal-Acoustic Velocimetry with Heterodyne Detection,” Opt. Lett. **25,** 224-226 (2000).

9 Hemmerling, B., D. N. Kozlov, and A. Stampanoni-Panariello, "Temperature and Flow-Velocity Measurements by Use of Laser-Induced Electrostrictive Gratings" Opt. Lett. **25,** 1340-1342 (2000).

10 R. C. Hart, G. C. Herring, and R. J. Balla, “Common-Path Heterodyne Laser-Induced Thermal Acoustics for Seedless Laser Velocimetry,” Opt. Lett. **27**, 710-712 (2002).

11 R. C. Hart, G. C. Herring, and R. J. Balla, “Pressure Measurement in Supersonic Air Flow by Differential Absorptive Laser-Induced Thermal Acoustics,” Opt. Lett. **32**, 1689-1691 (2007).

12 G. C. Herring, J. F. Meyers, and R. C. Hart, “Shock-Strength Determination with Seeded and Seedless Laser Methods,” Meas. Sci. Tech. 20, 045304 (2009).

13 G. C. Herring, “Mach Number Measurement with Laser and Pressure Probes in Humid Supersonic Flow,” AIAA Journal 46, 2107-2109 (2008).

14 J H. J. Eichler, P. GÜnter, and D. W. Pohl, *Laser-Induced Dynamic Gratings*, (Springer-Verlag, Berlin, 1986).

15 M. A. Buntine, D. W. Chandler, and C. C. Hayden, “Two-Color Laser-Induced Grating Technique for Gas-Phase Excited State Spectroscopy,” J. Chem. Phys. **97**, 707-710 (1992).

16 B. Hemmerling & A. Stampanoni-Panariello, “Imaging of Flames and Cold Flows in Air by Diffraction from a Laser-Induced Grating,” Appl. Phys. **B 57**, 281-285 (1993).

17 D. E. Govoni, J. A. Booze, A. Sinha, and F. F. Crim, “The Non-Resonant Signal in Laser-Induced Grating Spectroscopy of Gases,” Chem. Phys. Lett. **216**, 525-529 (1993).

18 E. B. Cummings, "Laser-Induced Thermal Acoustics: Simple Accurate Gas Measurements," Opt. Lett. **19**, 1361-1363 (1994).

19 R. Stevens and P. Ewart, “Single-Shot measurement of Temperature and Pressure using Laser-Induced Thermal Gratings with a Long Probe Pulse,” Appl. Phys. B **78**, 111–117 (2004).

20 R. C. Hart, R. J. Balla, and G. C. Herring, "Simultaneous Velocimetry and Thermometry of Air Using Nonresonant Heterodyned Laser-Induced Thermal Acoustics," Appl. Opt. **40**, 965-968 (2001).

21 R. C. Hart, R. J. Balla, and G. C. Herring, “Nonresonant Referenced Laser-Induced Thermal Acoustics Thermometry in Air,” Appl. Opt. **38**, 577-584 (1999).

22 H. E. Bass, L. C. Sutherland, J. Piercy, and L. Evans, “Absorption of Sound by the Atmosphere,” in Physical Acoustics, W. P. Mason and R. N. Thurston, eds. (Academic, Orlando, Fla.), Vol. 17, pp. 145–232 (1984).

23 G. C. Herring, “Temperature and Pressure Dependence of Signal Amplitudes for Electrostriction Laser-Induced Thermal Acoustics,” NASA Report TM-2015-218762 (May 2015).

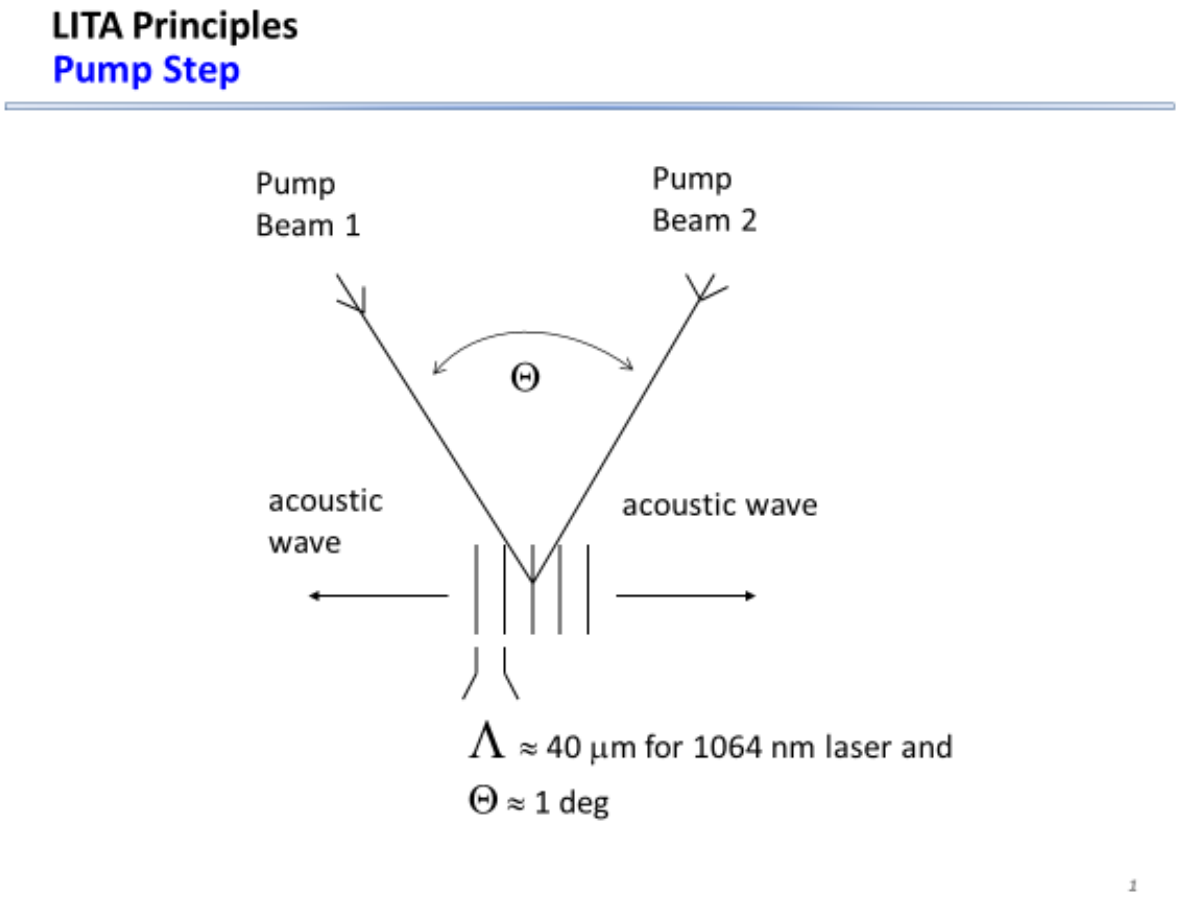

Figure 1a Schematic of two crossed pump-laser beams that are pulsed on for 10 ns, and the two counter-propagating sound wave packets that are generated.

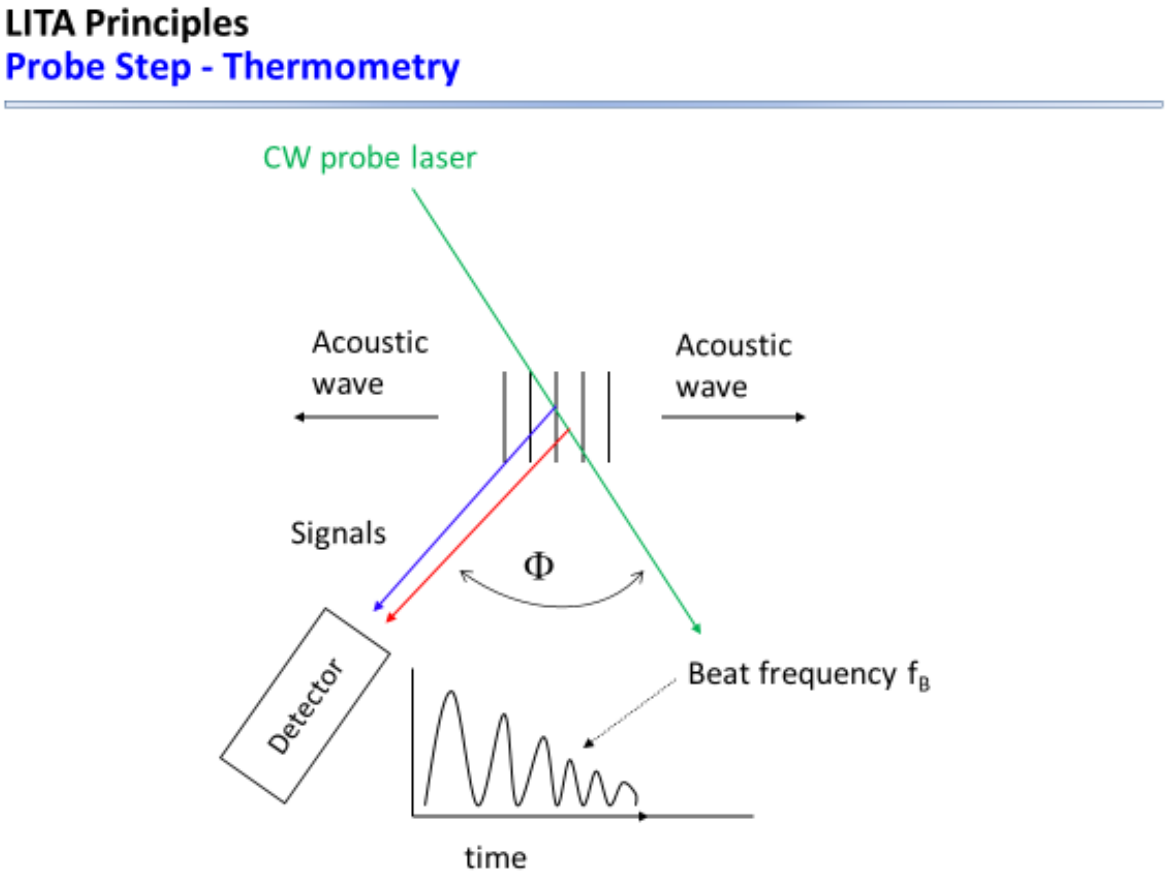

Figure 1b (Figure 1 continued) Schematic of the time dependence of the detector current from the Bragg reflections (red and blue) off of the two counterpropagating wave packets (black), from a third continuous laser beam (green).

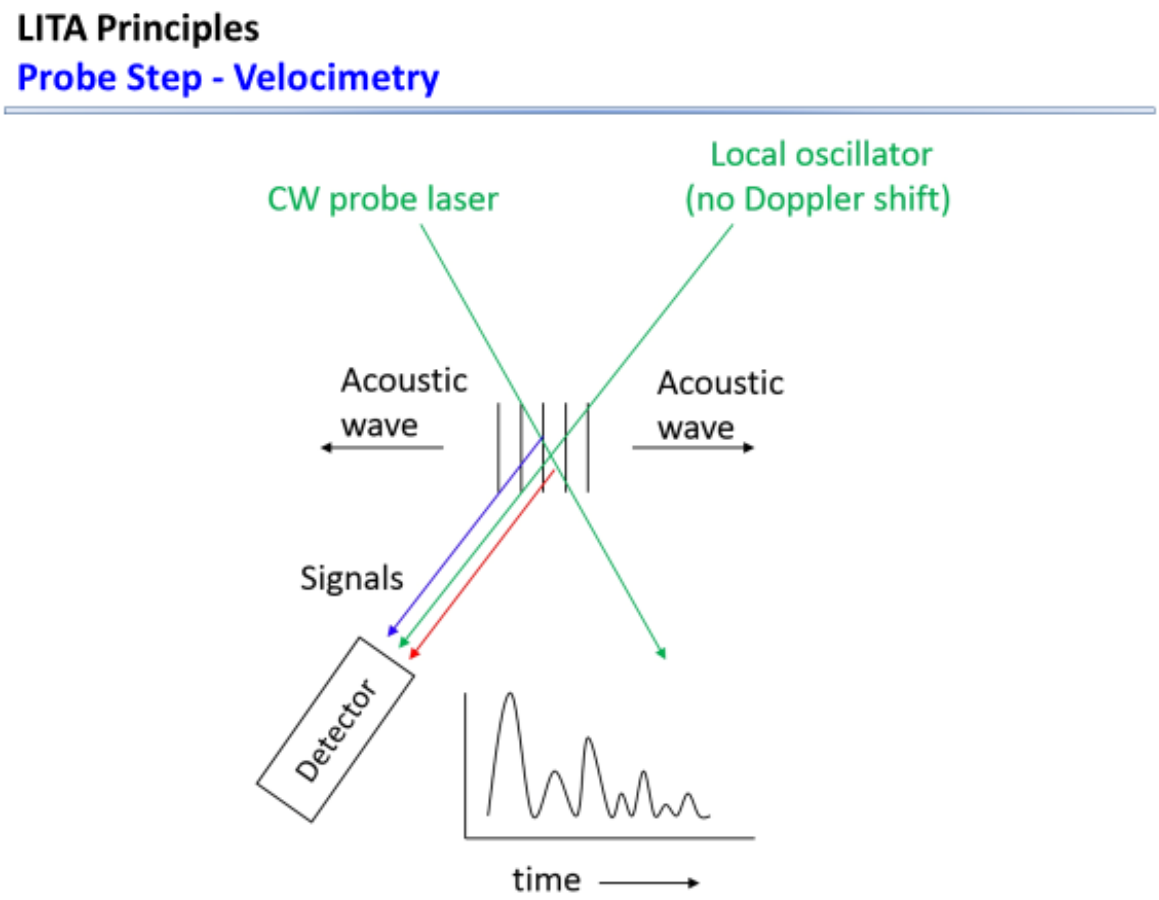

Figure 1c (Figure 1 concluded) Schematic of the time-evolving Bragg scattering (that includes three primary frequency components) generated from a more-complicated optical heterodyning of the Bragg reflections (red and blue) and a LO beam (green) on the detector photo-cathode surface.

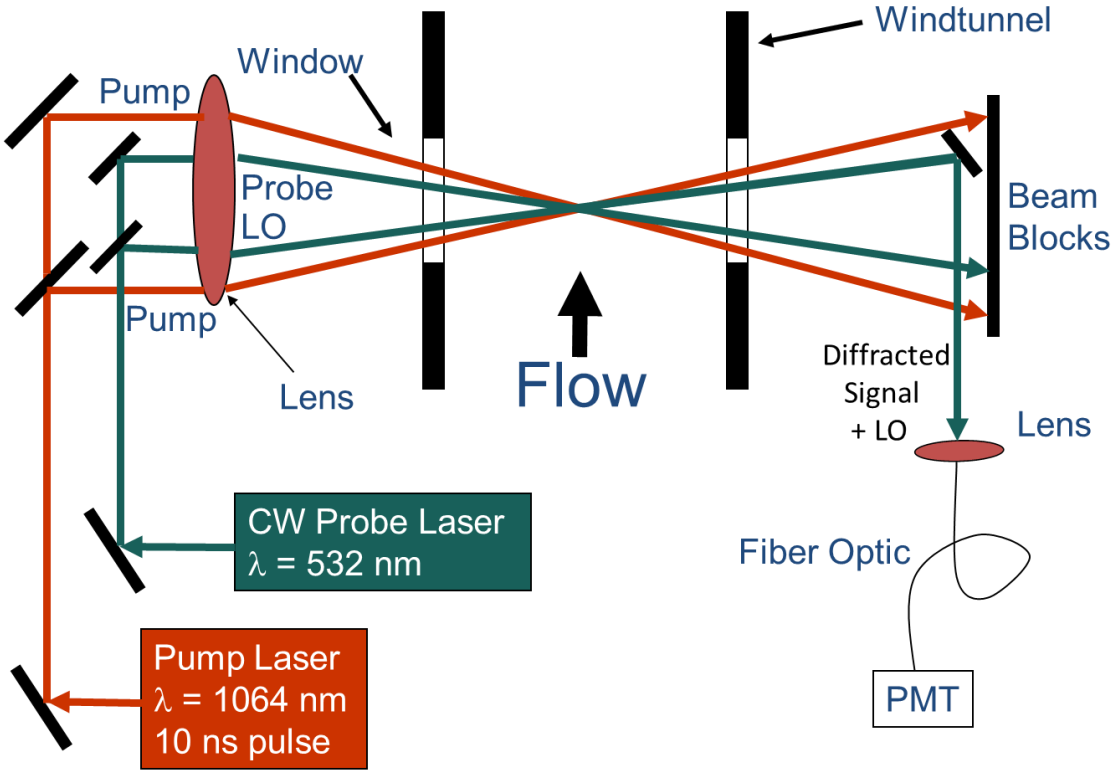

Figure 2 LITA setup schematic for Mach-2 freestream flow at SWT. Temperature measurement requires only input three beams, the probe and two pumps, while Mach-number measurement requires the addition of the fourth LO input beam.

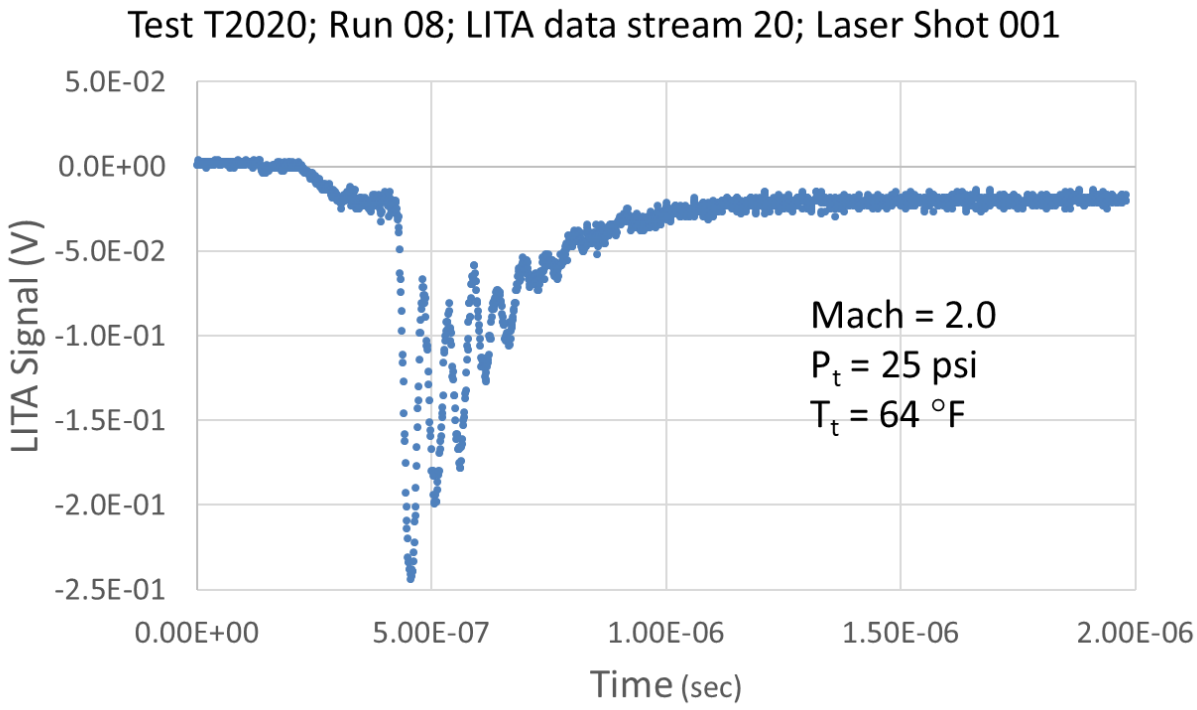

Figure 3 Typical single-laser-shot raw temporal LITA data (without the 4th input LO beam) from the SWT freestream, used for a temperature meaurement. Table 1 in Section IV shows a comparative summary of the run conditions for all data in Figs. 3-6 and 9, including all of the various units that appear in this report.

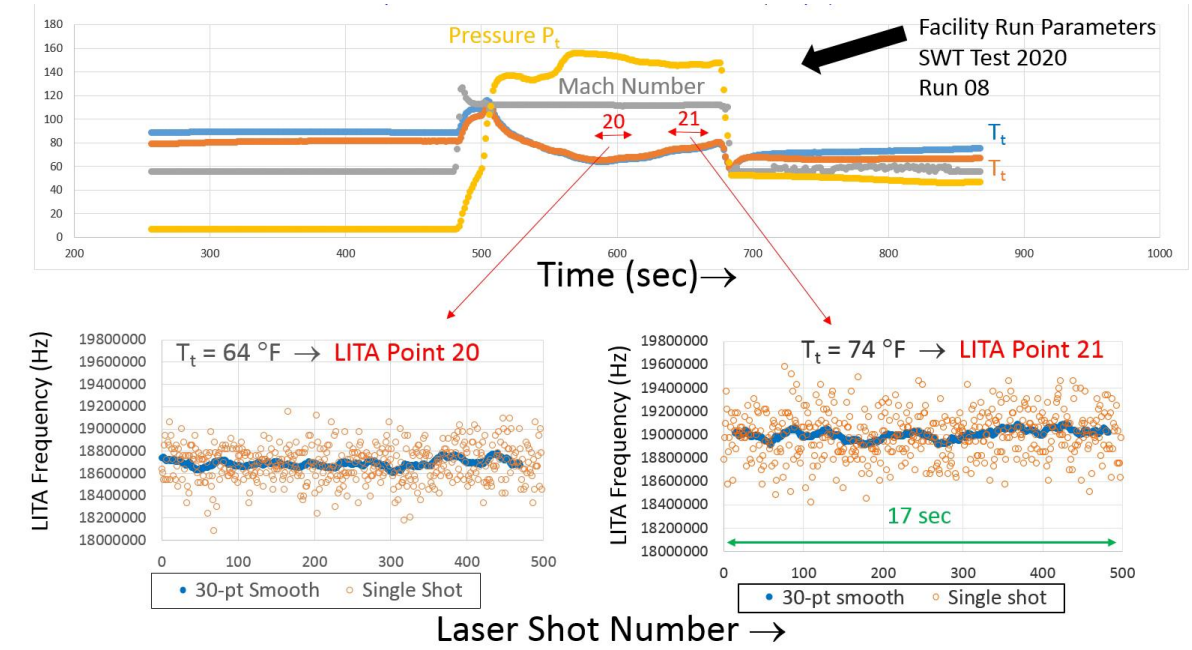

Figure 4 A 600-s history of four SWT flow parameters (upper panel) for a single run (SWT Test T2020, SWT Run 08). There is ≈ 100 s of useable runtime (maximum plateau of yellow P_t curve) that includes two sequential 17-s data-streams (lower panel) of LITA-measured-frequencies. Locations of the two LITA data-streams within the 100-s interval are denoted by red double-headed arrows, labeled Points 20 and 21 in both the upper and lower panels. Each individual open symbol (gold circles) is the LITA frequency determined by a discrete Fourier transform from a single laser pulse, while the filled blue circles show a running 30-laser-shot (1-s) smoothing.

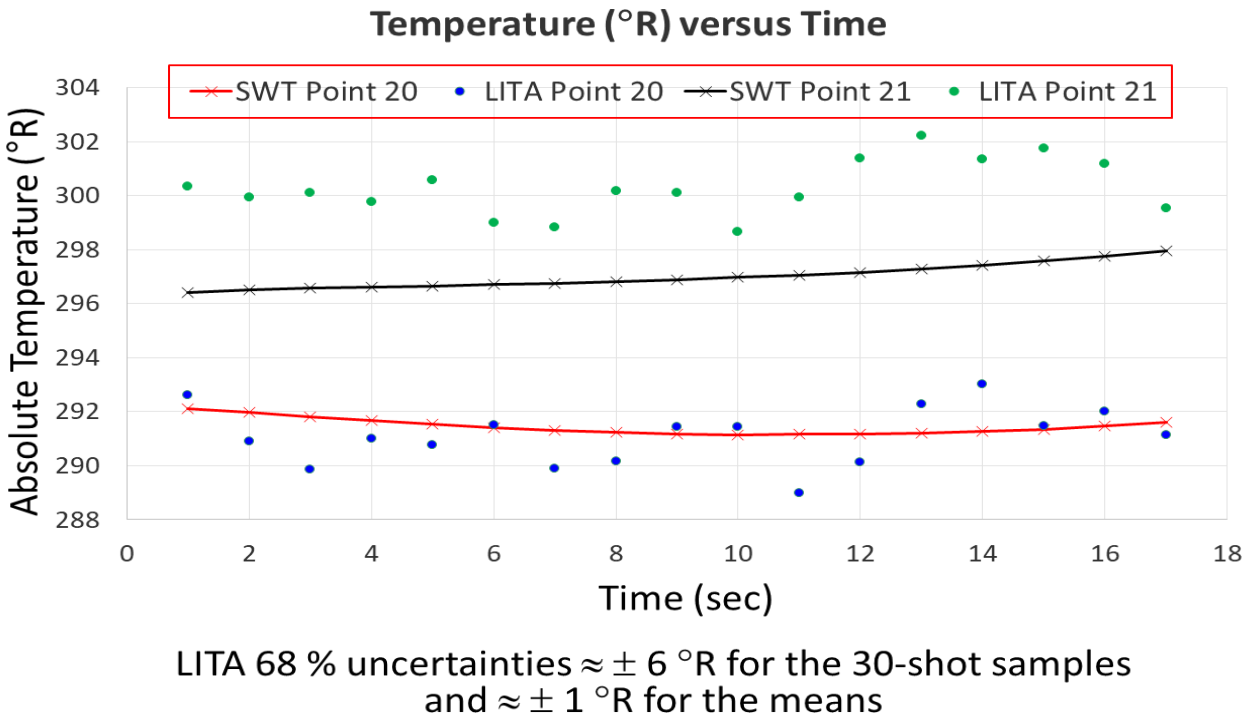

Figure 5 Comparison of freestream static temperatures for SWT facility probe-based values (red and black curves and stars) to LITA 30-laser-shot (1-s) averages (individual blue and green symbols) for LITA Points 20 and 21 of the single SWT Run 08 of Fig. 4. The 1-s standard deviations of the 1-s LITA means are about 0.3%, i.e., about ± 1 °R.

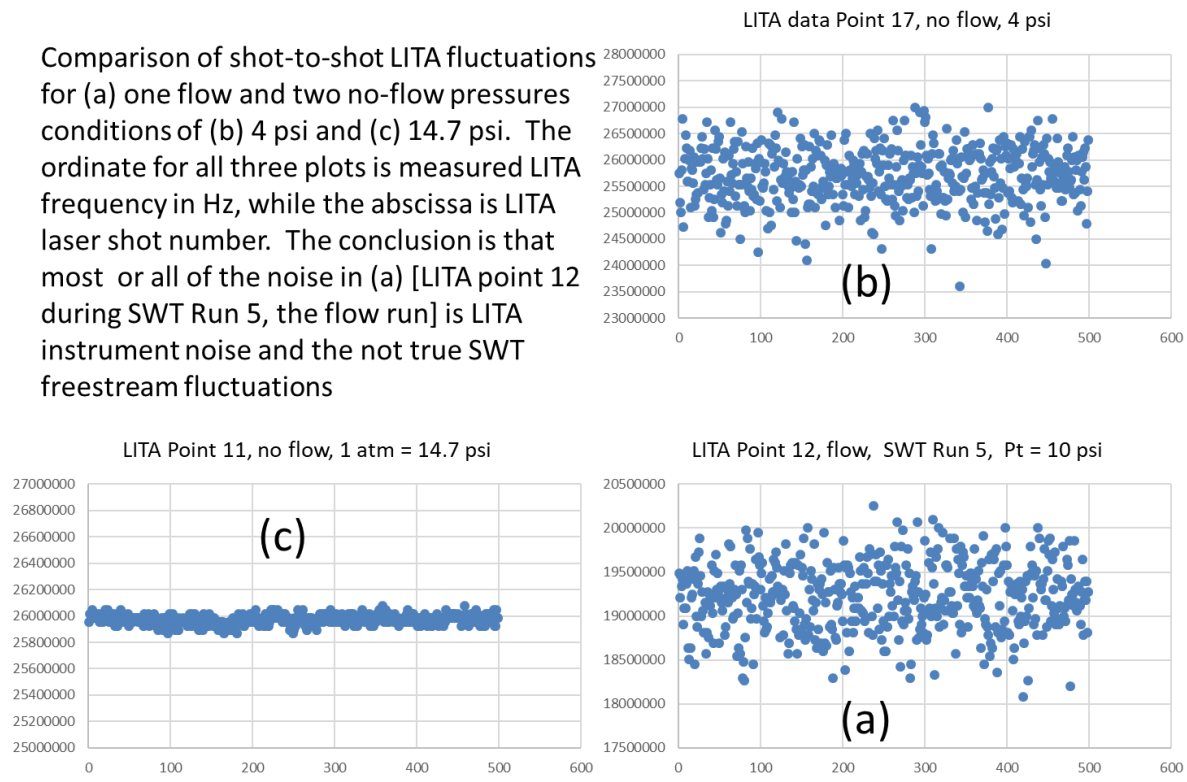

Figure 6 Comparison of shot-to-shot fluctuations of LITA-measured frequencies in Hz (i.e., square root of temperature) for three gas conditions: (a) Mach-2 flow at static pressure 1.4 psi, (b) no flow at 4 psi, and (c) no flow at 14.7 psi. Note the three different ordinate scales for the three parts.

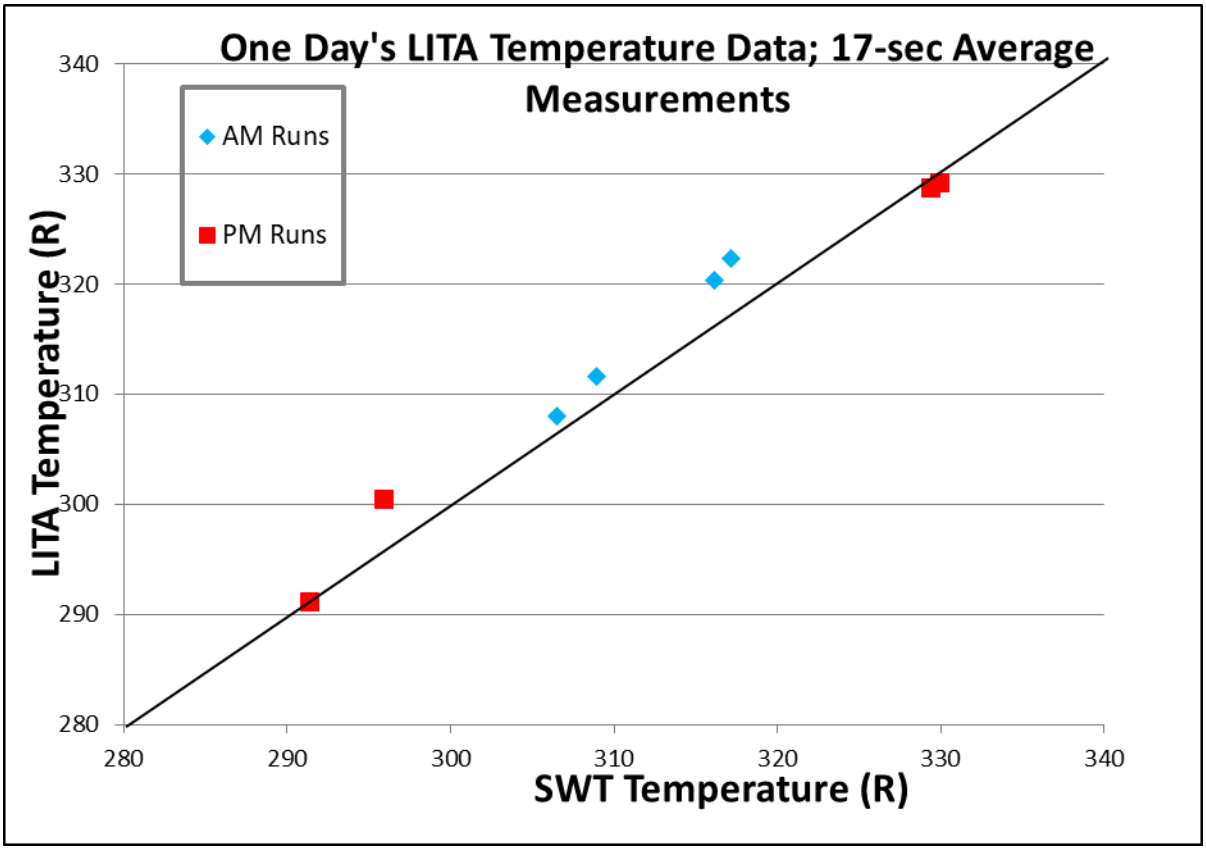

Figure 7a Comparison of freestream static temperatures of one-full-day's LITA 17-s averages (i.e., eight LITA points over four SWT runs on Day 1) to the expected probe-based SWT facility static-temperature values.

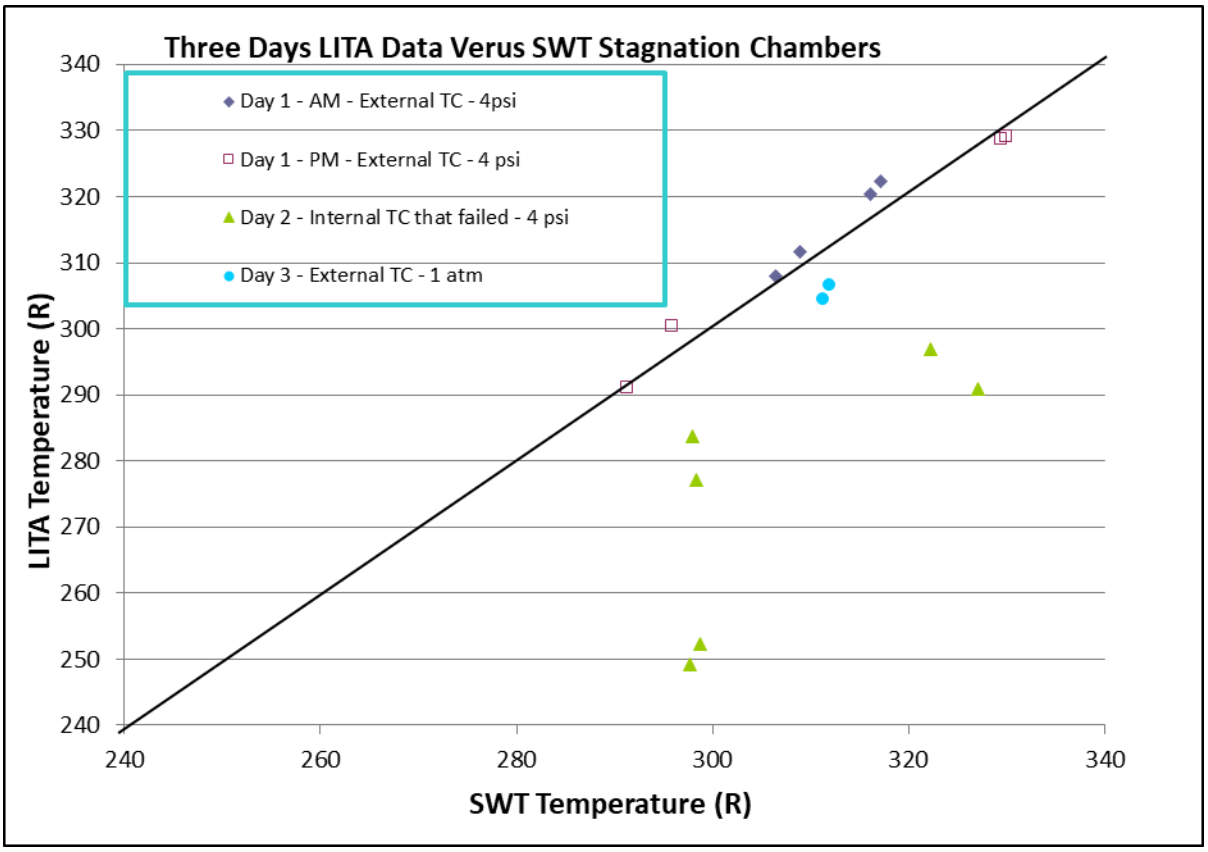

Figure 7b (Figure 7 concluded) Comparison of facility flow static temperatures for all three-day's LITA 17-s averages made over eight SWT runs. LITA calibration TCs that were external to the test section were used on Day 1 (open red squares and filled purple diamonds) and Day 3 (filled blue circles), whereas a TC inside the test section was used on Day 2 (filled green triangles). Day-2 LITA values are ~ 10% low due to the partial failure of the internal SWT probe TC (located inside the test section on the adjustable probe strut), that was used for calibration of the LITA instrument only on Day 2.

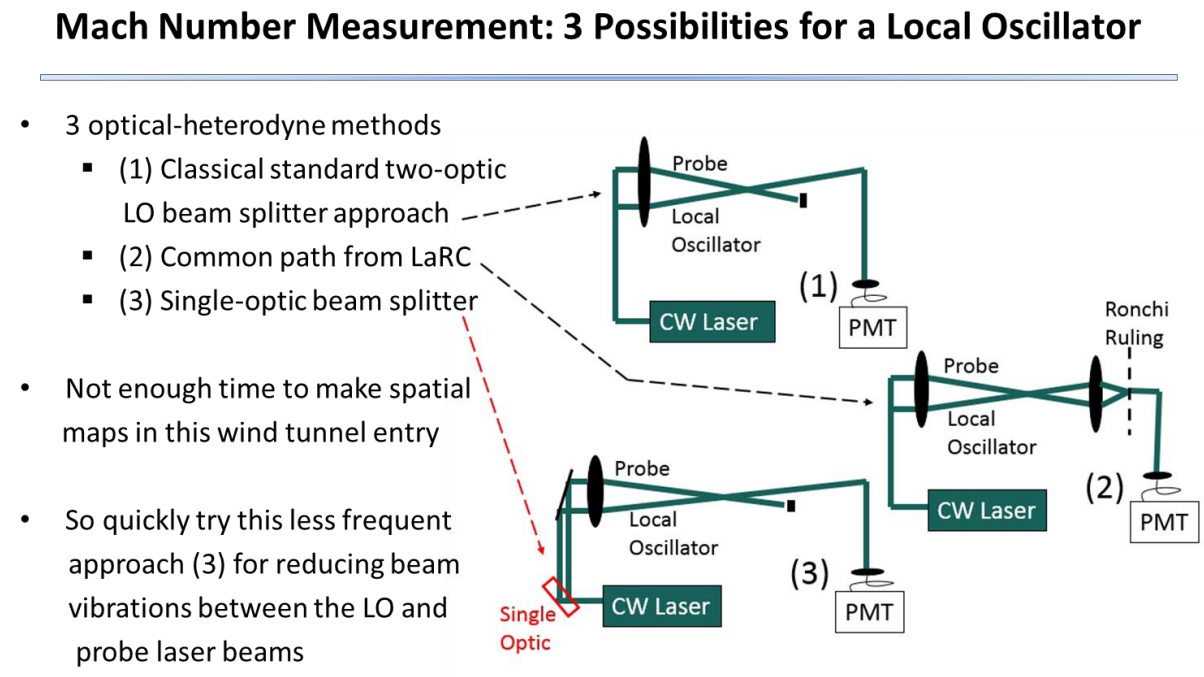

Figure 8 Comparison of three methods of beam-splitting and heterodyning, for LITA appartuses that may face vibration-challenging enviroments. The two crossed pump-laser beams are omitted for clarity of the different heterodyne schemes.

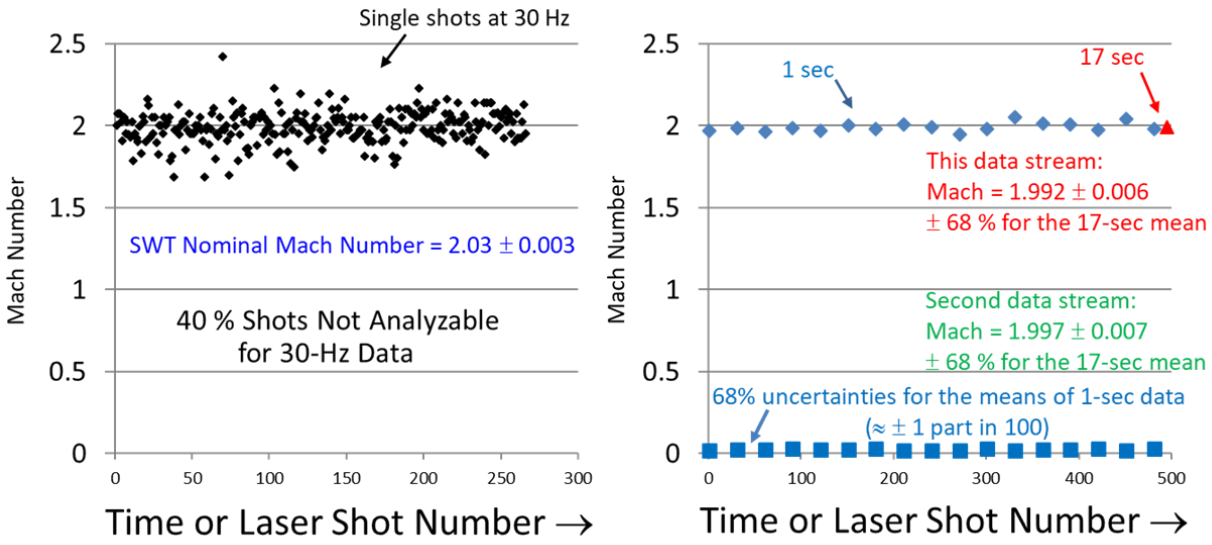

Figure 9 Example of single shot (black dots in left panel), 1-s average (blue diamonds in right panel), and 17-s average (red triangle in right panel) LITA Mach-number measurements, for a single LITA point (i.e., a 17-s, 500-laser-shot data stream). The standard deviations of the 1-s means are shown (blue squares in right panel). The result of a second LITA point (taken 20 s after the first point during the same tunnel run) is annotated in green text.

REPORT DOCUMENTATION PAGE

Form Approved
OMB No. 0704-0188

1. REPORT DATE *(DD-MM-YYYY)*	2. REPORT TYPE	3. DATES COVERED *(From - To)*
01-09-2020	TECHNICAL MEMORANDUM	

4. TITLE AND SUBTITLE

Freestream Mach-Number and Temperature Measurement in NASA Langley's 20-Inch Supersonic Wind Tunnel Using Laser-Induced Thermal Acoustics

5a. CONTRACT NUMBER

5b. GRANT NUMBER

5c. PROGRAM ELEMENT NUMBER

6. AUTHOR(S)

Herring, Gregory C.; Balla R. Jeffrey; Beeler, George B.

5d. PROJECT NUMBER

5e. TASK NUMBER

5f. WORK UNIT NUMBER

081876.02.07.40.40.01

7. PERFORMING ORGANIZATION NAME(S) AND ADDRESS(ES)

NASA Langley Research Center
Hampton, VA 23681-2199

8. PERFORMING ORGANIZATION REPORT NUMBER

9. SPONSORING/MONITORING AGENCY NAME(S) AND ADDRESS(ES)

National Aeronautics and Space Administration
Washington, DC 20546-001

10. SPONSOR/MONITOR'S ACRONYM(S)

NASA

11. SPONSOR/MONITOR'S REPORT NUMBER(S)

NASA-TM-2020-5007323

12. DISTRIBUTION/AVAILABILITY STATEMENT

Unclassified - Unlimited
Subject Category
Availability: NASA STI Program (757) 864-9658

13. SUPPLEMENTARY NOTES

14. ABSTRACT

We report single-laser-shot (0.3 microseconds) and time-averaged (30 Hz repetition rate) measurements of static temperature T and Mach number M in the freestream of NASA Langley's 20-inch Supersonic Wind Tunnel (SWT), using a nonintrusive optical technique: laser-induced thermal acoustics (LITA). The 1-s averages only provide upper limits for the temporal stability of the freestream tunnel flow on 1-s time scales and complement previous work that characterized the SWT spatial uniformity of the flow. They also provide a first noninvasive comparison to the traditional calibrations with physical probes, for both the mean and fluctuating components of the freestream.

15. SUBJECT TERMS

Laser-Induced Thermal Acoustics (LITA); 20-Inch Supersonic Wind Tunnel (SWT); Freestream Measurement; Mach Number; Temperature

16. SECURITY CLASSIFICATION OF:			17. LIMITATION OF ABSTRACT	18. NUMBER OF PAGES	19a. NAME OF RESPONSIBLE PERSON
a. REPORT	b. ABSTRACT	c. THIS PAGE			HQ - STI-infodesk@mail.nasa.gov
U	U	U	UU	50	19b. TELEPHONE NUMBER *(Include area code)* 757-864-9658